A Physics-informed Convex Data Driven Model for Grid-interactive Reverse Osmosis Desalination Plant

Naveen Jagadeesan
Department of Mechanical Engineering
Texas A&M University
College Station, TX, USA
naveen_jagadeesan@tamu.edu

Mucun Sun
Idaho National Laboratory
Idaho Falls, ID, USA
Mucun.Sun@inl.gov

Nima Fathi, Guanyu Tian
Department of Marine Engineering Technology
Texas A&M University
Galveston, TX, USA
{nfathi, tiang}@tamu.edu

***Abstract*—Reverse osmosis (RO) desalination plants can serve as flexible electrical loads that enhance grid demand response and support reliable operation of data-center-driven communities. However, accurate and computationally efficient modeling of RO dynamics remains challenging due to nonlinear coupling among flow, pressure, solute transport, and membrane flux. This paper develops a physics-informed convex modeling framework that combines high-fidelity numerical simulation with machine learning. A two-dimensional finite-difference RO model generates synthetic data across operating pressures and flow rates, capturing freshwater flux and power consumption behavior. An Input Convex Neural Network (ICNN) surrogate enforces convexity with respect to physical inputs, ensuring both interpretability and numerical stability. The resulting hybrid model achieves near-simulation accuracy at a fraction of the computational cost, enabling real-time optimization and integration of RO plants into grid scheduling. This framework supports coordinated water-energy management for communities hosting high-density data centers and other flexible demand resources.**

***Index Terms*—Demand response, desalination, physics-informed learning, neural networks.**

I. Introduction

Human civilization has been fundamentally nurtured and shaped by freshwater resources. The distribution of freshwater has long determined where societies could emerge and prosper, forming the ecological and economic backbone of human development. In the modern era, this interdependence between water and prosperity has intensified. The rapid expansion of data centers and other energy-intensive infrastructures, which are pivotal to digital and economic growth with high demand for freshwater, has further tightened the water–energy–economy nexus, underscoring the strategic importance of sustainable and resilient freshwater management and generation [1].

Among all alternative freshwater generation methods, Reverse osmosis (RO) desalination is the most widely adopted alternative freshwater technology due to its scalability and energy efficiency [2]. However, its operational cost is dominated by electricity consumption, with desalination costs reported up to 115% and 20% higher than conventional treatment for seawater and brackish water, respectively [3]. Moreover, large desalination facilities can introduce high peak electrical loads that affect grid reliability and local electricity prices, particularly in constrained grids [4].

Flexible control of RO plants provides an opportunity to better integrate water and energy systems at the community level [5]. By coordinating RO power consumption with grid conditions, desalination plants can reduce infrastructure upgrade needs and participate in demand response and ancillary service markets. This capability improves grid resilience against renewable intermittency while reducing both power system operating costs and freshwater production expenses.

Despite this potential, grid-integrated control and optimization of RO plants are challenging due to modeling complexity. RO dynamics involve nonlinear coupling among pressure-driven transport, solute rejection, concentration polarization, and pressure loss along the membrane channel [6]. Numerical models based on finite difference or finite volume methods provide high fidelity but are computationally expensive for long-channel simulations [7]. Analytical correlations offer simpler relationships but lack generality across operating conditions [8].

To overcome these limitations, machine learning approaches have recently been introduced for RO modeling. Conventional neural networks and regression-based models can approximate flux and energy performance from operational data [9]. However, many of these models suffer from overfitting, limited interpretability, and a lack of physical consistency—for example, failing to guarantee convex flux with pressure. Such shortcomings restrict their reliability in optimization and real-time control applications.

In this work, we present a hybrid modeling framework that combines the rigor of physics-based simulation with the efficiency of machine learning. A high-fidelity RO simulator that can capture long-channel behavior under different velocities and pressures was developed in Python to generate the synthetic dataset. An Input Convex Neural Network (ICNN) embedding convexity constraints was trained to learn the physical model and predict the power and flux of freshwater in alignment with physical laws. This integrated approach delivers both accuracy and computational efficiency, enabling its use in optimization and digital twin applications for RO desalination systems. The contributions of this paper are three-fold: 1) a high-fidelity physics-based RO model is developed to simulate the desalination process and assess the grid-related variables; 2) a synthetic dataset is generated for the training of data-driven RO models; and 3) implementation of an input convex neural network (ICNN) as an accurate and computationally efficient grid integration model for RO desalination plants.

This paper is organized as follows. Section II develops the physics-based numerical model, including the governing

979-8-3315-8138-1

equations for coupled fluid flow and solute transport, analytical expressions for freshwater flux and electric power consumption under varying operating pressures and flow rates. Section III introduces the data-driven modeling framework, where an Input Convex Neural Network (ICNN) is implemented to learn the physically consistent relationship between operating parameters, freshwater generation, and energy demand. Section IV provides a case study to validate the proposed approach, demonstrating the performance of both the physics-based and ICNN surrogate models under practical operating conditions. Finally, Section V concludes the paper and discusses future directions.

II. Physical Modeling of the Reverse Osmosis Process

In this section, we develop the numerical simulation model of a typical reverse osmosis (RO) process to get the freshwater flux and electric power consumption under different operation conditions of pressure and flow rate. The RO process is a two-dimensional coupled fluid flow and solute transport problem. The feed solution flows through a spiral channel bounded by semi-permeable membranes, which define the permeate boundaries. The computational model resolves both the hydrodynamic and solute concentration fields under steady or transient operating conditions. We solve this problem using an explicit time-stepping approach with finite-difference spatial discretization to capture the evolution of velocity, pressure, and concentration according to the governing equations for mass, momentum, and solute transport.

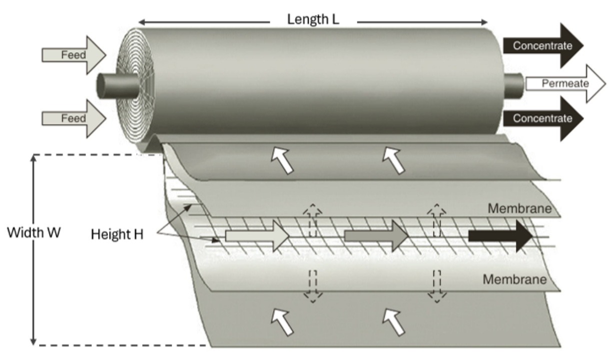

Fig. 1. Schematic of a typical RO channel.

As Fig. 1 shows, the modeled RO channel has a length L, height H, and width W (into the page) [10]. Flow is oriented along the x-axis, while solute and velocity gradients are normal to the membrane and vary along y. The channel space is discretized into N_x and N_y uniformly spaced grid points as formulated in (1), where Δx and Δy denote the intervals on the x and y axis respectively. These uniform intervals minimize spurious diffusion and simplify boundary condition enforcement in the finite-difference scheme, as supported by prior CFD studies of RO feed channels.

$$\Delta x = \frac{L}{N_x - 1}, \quad \Delta y = \frac{H}{N_y - 1} \tag{1}$$

A. Governing Equations

The physics constraints of the process are the coupled conservation equations for mass, momentum, and solute transport. The field state variables, including the x and y axis velocity components v_x, v_y, pressure p, and solute concentration C, are iteratively updated to ensure hydrodynamic consistency and solute coupling.

The feed-side flow is described by the incompressible, steady-state Navier–Stokes equations in (2), where ρ denotes the density of the fluid.

$$\rho\left(v_x\frac{\partial v_x}{\partial x} + v_y\frac{\partial v_x}{\partial y}\right) = -\frac{\partial p}{\partial x} + \mu\left(\frac{\partial^2 v_x}{\partial x^2} + \frac{\partial^2 v_x}{\partial y^2}\right) \tag{2a}$$

$$\rho\left(v_x\frac{\partial v_y}{\partial x} + v_y\frac{\partial v_y}{\partial y}\right) = -\frac{\partial p}{\partial y} + \mu\left(\frac{\partial^2 v_y}{\partial x^2} + \frac{\partial^2 v_y}{\partial y^2}\right) \tag{2b}$$

The Navier-Stokes equations are discretized on a structured Cartesian grid using a finite-difference approach. The non-linear convective terms are approximated using a first-order upwind scheme to ensure numerical stability in the long, high-aspect-ratio RO feed channel. For a generic transported velocity component $\phi \in \{u, v\}$, the axial convective term is discretized based on the sign of the local advecting velocity as (3)

$$u\frac{\partial \phi}{\partial x}\Big|_{i,j} \approx \begin{cases} u_{i,j}\dfrac{\phi_{i,j} - \phi_{i-1,j}}{\Delta x}, & u_{i,j} \geq 0, \\ u_{i,j}\dfrac{\phi_{i+1,j} - \phi_{i,j}}{\Delta x}, & u_{i,j} < 0, \end{cases} \tag{3}$$

The continuity constraint (4) is also enforced to maintain the conservation of mass.

$$\frac{\partial v_x}{\partial x} + \frac{\partial v_y}{\partial y} = 0 \tag{4}$$

The incompressibility characteristic of the fluid is enforced using a pressure–Poisson correction that couples the velocity and pressure fields at each time step [11]. It also enhances the numerical stability of the simulation.

The transient transport of solute concentration $C(x, y, t)$ is governed by (5).

$$\frac{\partial C}{\partial t} + v_x\frac{\partial C}{\partial x} + v_y\frac{\partial C}{\partial y} = D\left(\frac{\partial^2 C}{\partial x^2} + \frac{\partial^2 C}{\partial y^2}\right) \tag{5}$$

where D is the diffusivity of NaCl in water. Both advection and diffusion terms are discretized explicitly, with upwind differencing applied when local velocity components are nonzero to prevent unphysical oscillations.

B. Freshwater Generation Model

The freshwater flux J_w through the membrane follows the solution–diffusion model (6).

$$j_w = A(\Delta P - \Delta\pi) \tag{6}$$

where A is the hydraulic permeability constant, ΔP is the transmembrane pressure difference, and $\Delta\pi$ is the local osmotic pressure difference opposing permeation, which is proportional to the solute concentration C at the point.

The total freshwater generation rate J_w is the integration of freshwater flux j_w along the length. Its discretized implementation is formulated in (7), where $j_{w,i}$ denotes the flux at the i^{th} interval.

$$J_w = \sum_{i=1}^{N_x} j_{w,i} \tag{7}$$

C. Membrane Interface and Water Flux

The semi-permeable nature of the RO membrane is incorporated directly into the flow solver through a wall-normal velocity boundary condition derived from the permeate flux. At the membrane surfaces, the normal velocity component is prescribed as (8).

$$v_y\big|_{\text{membrane}} = -J_w \tag{8}$$

where J_w is the locally computed transmembrane water flux obtained from the solution–diffusion model. This boundary condition represents the volumetric removal of fluid through the membrane and is enforced prior to the pressure–Poisson projection step.

D. Power Consumption Model

The overall electrical power consumption of the RO desalination process is formulated as a function of the volumetric feed flow rate Q and recovery ratio η as in (9) [12]. The electrical power required, P_{elec}, represents the energy consumed by the pump to deliver pressurized saline feedwater to the membrane channel, and is defined as follows:

$$P_{\text{elec}} = \frac{Q(P_{\text{oper}} + \Delta P_{\text{loss}})}{\eta} \tag{9}$$

where Q is the volumetric feed flow rate in m^3/s, P_{oper} is the applied operating pressure in pascals (Pa), ΔP_{loss} denotes the frictional pressure loss along the feed channel in pascals, and η characterizes the pump efficiency or system recovery ratio, a dimensionless number representing the fraction of the pump energy converted into useful pressure.

The volumetric feed flow rate, Q is

$$Q = U_{\text{in}} H W \tag{10}$$

where U_{in} is the inlet velocity of the feed solution (m/s), H is the channel height (m), and W is the channel width (m).

E. Data Generation

The above physics-based models are implemented in Python to generate synthetic data for the training and validation of the convex machine learning models in section III. Dynamic boundary coupling between pressure-driven flow, osmotic resistance, and solute buildup is adopted to yield an accurate portrayal of membrane-channel interactions under operational RO conditions.

The implementation structure of the simulation follows Algorithm 1, where ε denotes the L2 norm of the relative change between successive sampling times of the velocity and pressure fields.

Algorithm 1 Numerical Solver for RO Module Simulation

- Initialize velocity, pressure, and concentration fields
- **for** each time step t **do**
    - Apply inlet boundary conditions: velocity u_{in}, concentration C_{in}
    - Solve Navier–Stokes equations via explicit time-stepping
    - Solve pressure-Poisson equation to enforce incompressibility
    - Solve advection-diffusion equation for salt concentration
    - **for** each membrane node (top and bottom) **do**
        - Estimate local osmotic pressure from concentration
        - Compute water flux J_w using fixed-point iteration
        - Update local concentration polarization model
    - **end for**
    - Record permeate flux and salt rejection at each membrane
    - Update global performance metrics: Recovery and Power
- **end for** Steady-State Convergence: $\varepsilon \leq 10^{-3}$.
- Output simulation results

III. Implementation of ICNN to RO Desalination System Modeling

In reverse osmosis (RO) desalination, predicting permeate (freshwater) flux under varying operating conditions is critical for optimizing energy efficiency and water recovery. While high-fidelity physics-based simulators accurately model these dynamics, they are computationally expensive and unsuitable for rapid evaluation or optimization. Neural networks offer a promising alternative, but traditional architectures lack physical consistency and may produce non-convex predictions, especially when extrapolating beyond the training range.

To address these limitations, we propose using an Input Convex Neural Network (ICNN) as a surrogate model that predicts permeate flux based on key operating conditions. The ICNN enforces convexity with respect to selected inputs, aligning its behavior with known physical relationships and ensuring interpretability and robustness. This makes it particularly attractive for integration into optimization and control workflows in desalination systems.

A. ICNN Architecture and Physical Motivation

The Input Convex Neural Network (ICNN) used in this study is designed to incorporate physical constraints derived from reverse osmosis (RO) transport principles by enforcing convexity on select operational inputs. In the implemented model, the input space is divided into two distinct subsets based on their physical relationships to permeate flux: *convex inputs* and *non-convex inputs*.

The **convex inputs** include the *feed velocity* (U_{in}) and *operating pressure* (P_{oper}), which are known to have a monotonic influence on water flux in RO systems. As pressure and velocity increase, the transmembrane driving force and shear-induced mass transfer both enhance permeate flux. Therefore, these variables are modeled under convex constraints to ensure

979-8-3315-8138-1

that the network output (predicted flux) increases monotonically with them, consistent with physical expectations.

The **non-convex inputs**, such as *frictional pressure loss* (ΔP_{fric}) and *pump power consumption* (P_{elec}), are included to account for nonlinear system effects and energy dissipation. These variables influence secondary phenomena such as energy efficiency and recovery, making them suitable for the non-convex input stream.

In practice, the model accepts a four-dimensional input vector:

$$x = [U_{\text{in}}, P_{\text{oper}}, \Delta P_{\text{fric}}, P_{\text{elec}}]$$

and predicts the scalar target flux J_w obtained from physics-based simulations. The inputs are normalized using standard scaling to accelerate convergence during optimization.

The network architecture follows a partially input-convex configuration [13]. The ICNN is composed of two interconnected pathways: the *convex stream* (z-path) and the *non-convex stream* (u-path). The u-path processes non-convex variables through standard dense layers, while the z-path ensures convexity by applying non-negative weight constraints to connections from previous z-layers and ReLU activations to maintain convex behavior. The mathematical structure of the forward propagation is formulated in (11).

$$\begin{aligned} u_{i+1} &= \tilde{g}_i\left(\tilde{W}_i u_i + \tilde{b}_i\right), \\ z_{i+1} &= g_i\left(W_i^{(zu)} u_i + W_i^{(zz)} z_i + b_i\right), \quad W_i^{(zz)} \geq 0, \\ f(x;\theta) &= z_k, \end{aligned} \tag{11}$$

where $g_i(\cdot)$ and $\tilde{g}_i(\cdot)$ are ReLU activations, ensuring that the final output $f(x;\theta)$ remains convex in the designated convex inputs. The non-negativity constraint on $W_i^{(zz)}$ is enforced internally through a ReLU transformation (`ReLU(`W`)`), guaranteeing convexity throughout training.

This formulation allows the ICNN to preserve the expected physical monotonicity of flux with respect to pressure and velocity, while still capturing the nonlinear interactions arising from hydraulic losses and power input. Consequently, the resulting model acts as a physics-guided surrogate capable of providing accurate, interpretable, and computationally efficient flux predictions across diverse operating conditions.

B. ICNN Training

The ICNN is trained with the dataset generated from the simulation of the physics-based RO solver introduced in section II with varied parameters. The feed pressure and velocity vary across the practical operating ranges 40–70 bar and 0.1–0.5 m/s, while the salinity, temperature, and geometry are kept constant. Each simulation run produced outputs including permeate flux (J_w) and power consumption.

The supervised learning strategy is adopted with the loss function (12), where the mean squared error between predicted and simulated flux values is minimized.

$$\mathcal{L}(\theta) = \frac{1}{N}\sum_{i=1}^{N}\left(f(x^{(i)}, y^{(i)};\theta) - J_w^{(i)}\right)^2 \tag{12}$$

Training was conducted using the Adam optimizer with early stopping based on validation performance. The weights in the convex input path were reparameterized to non-negative to ensure the convexity relationship between the convex inputs and the network output. This approach ensured not only accuracy but also physical consistency in the model outputs.

IV. Case Study

In this section, we present a simulation-based case study of a real-world reverse osmosis (RO) desalination plant to validate the effectiveness of the physics-based numerical model and the performance of the ICNN-based data-driven model. The simulations are carried out in Python on a desktop computer with a 2.5 GHz 6-core CPU and 32 GB of memory.

A. Settings

The simulated RO model is a digital twin model of the commercial spiral-wound elements [14]. The channel geometry is approximated as a narrow feed spacer region bounded by two parallel membranes. A summary of the geometric and physical parameters used in the model is provided in Table I.

TABLE I
Geometry and Operating Parameters for Data Generation

Parameter	Symbol	Value / Range
Channel Length	L	1.0 m
Channel Height	H	700 μm
Channel Width	W	1.0 m
Feed Velocity	U_{in}	0.1–0.5 m/s
Operating Pressure	P_{oper}	40–70 bar
Feed Salinity	C_{feed}	35,000 ppm
Temperature	T	25°C
Membrane Permeability	A	Assumed constant

B. Numerical Model Performance

The internal flow dynamics of the velocity field within the feed channel play a critical role in determining both the power consumption and freshwater flux of the system. In this section, we we consider a representative scenario with an inlet velocity of 0.3 m/s and an applied pressure of 60 bar to present the effectiveness of the high-fidelity numerical model of the reverse osmosis (RO) desalination process.

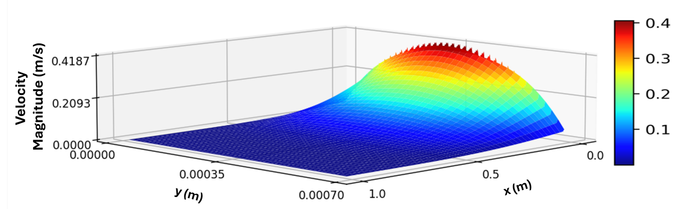

Fig. 2. Velocity magnitude and flow pattern inside the channel

The internal flow velocity map is depicted in Fig. 2, where the maximum velocity is observed near the inlet and in the central region, consistent with the targeted inlet velocity ($\sim 0.42\,\text{m/s}$). The direction field highlights the efficient flow establishment and boundary effects. It can be learned from the gradients of the internal states that as feed water flows downstream, pressure drops due to frictional losses and salt

979-8-3315-8138-1

accumulates at the membrane interface, leading to a gradual decline in local flux.

The numerical results are consistent with reported experimental and pilot-scale seawater RO systems. The inlet velocity range and operating pressures considered in this work align with the experimental SWRO studies [9]. The predicted permeate flux and its sensitivity to pressure and feed conditions fall within the ranges reported for spiral-wound RO modules operating at comparable salinity and temperature [15].

C. ICNN Surrogate Model Performance

The performance of the ICNN-based surrogate model was evaluated by comparing its predictions against the physical model results under the testing set randomly drawn from the entire dataset. Fig. 3 illustrates the ability of the trained ICNN to accurately predict RO module water flux across the testing set. Numerical results shows almost all prediction errors are contained within $\pm 1\%$ of the benchmark values. The overlayed normal distribution and narrow error bounds highlight the model's accuracy and reliability for RO energy intake and freshwater output predictions.

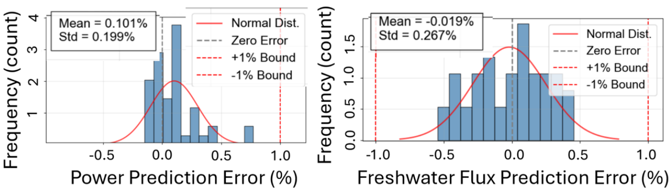

Fig. 3. Distribution of ICNN prediction errors for power and fresh water flow rate

Besides the modeling accuracy, the high computational efficiency is also a strength of data-driven methods. The average run time of the high-fidelity physics-based RO simulator and the ICNN-based surrogate model as well as ther standard deviations over the testing cases are compared in Table II. While the full numerical model requires over 900 seconds per sample due to the complexity of solving the coupled Navier–Stokes and advection–diffusion equations at fine spatial resolutions, the trained ICNN surrogate predicts freshwater flux and power consumption in less than 1 millisecond. This significant gain in speed allows the ICNN to perform real-time inference suitable for optimization and control tasks that would otherwise be computationally prohibitive using the physics model.

TABLE II
TIME EFFICIENCY COMPARISON

Model	Averge Time per sample (s)	Std
Physical Model	954.33	55.16
ICNN Surrogate	0.000318	0.00007

Despite its high accuracy and substantial speed-up, the ICNN model focuses solely on terminal conditions and does not capture the internal flow or solute dynamics within the RO channel. Therefore, it is not intended to replace physics-based models but rather to complement them in applications requiring rapid estimation of overall system performance, such as real-time control for grid-integrative RO desalination plants.

V. CONCLUSIONS

This paper developed a physics-informed convex data-driven framework that combines physics-based reverse osmosis (RO) model with an Input Convex Neural Network (ICNN) surrogate for fast estimation of desalination performance. By enforcing convexity with respect to key operational variables, the ICNN preserves the physical relationship between pressure, flow rate, freshwater flux, and power demand, while achieving high accuracy at several orders of magnitude lower computational cost. The surrogate model captures the demand-side behavior of an RO plant in a form that is directly compatible with optimization and control, providing a practical foundation for representing desalination systems as flexible, grid-interactive loads. Future work will extend this modeling framework to integrated grid-level case studies, where ICNN is embedded into scheduling and demand response optimization. In addition, validation with real plant measurements will be pursued through collaboration with industrial partners.

REFERENCES

[1] A. Shokri and M. S. Fard, "Techno-economic assessment of water desalination: Future outlooks and challenges," *Process Safety and Environmental Protection*, vol. 169, pp. 564–578, 2023.

[2] M. Qasim, M. Badrelzaman, N. N. Darwish, N. A. Darwish, and N. Hilal, "Reverse osmosis desalination: A state-of-the-art review," *Desalination*, vol. 459, pp. 59–104, 2019.

[3] S. Ebrahim and M. Abdel-Jawad, "Economics of seawater desalination by reverse osmosis," *Desalination*, vol. 99, no. 1, pp. 39–55, 1994.

[4] A. J. Garzon and L. A. Hierro, "Electricity price and inflation: Macroeconomic implications of real-time pricing," *The Energy Journal*, vol. 45, no. 4, pp. 195–222, 2024.

[5] K. Oikonomou and M. Parvania, "Optimal participation of water desalination plants in electricity demand response and regulation markets," *IEEE Systems Journal*, vol. 14, no. 3, pp. 3729–3739, 2019.

[6] H. Sitaraman and I. Battiato, "Impact of large-scale effects on mass transfer and concentration polarization in reverse osmosis membrane systems," *Separation and Purification Technology*, vol. 303, p. 122121, 2022.

[7] A. E. Anqi, N. Alkhamis, and A. Oztekin, "Computational study of desalination by reverse osmosis—three-dimensional analyses," *Desalination*, vol. 388, pp. 38–49, 2016.

[8] M. Özdinç Çarpinlioğlu and E. Özahi, "A simplified correlation for fixed bed pressure drop," *Powder Technology*, vol. 187, no. 1, pp. 94–101, 2008.

[9] E. Guler, J. Piekacz, D. Ozakdagc, W. Kujawski, M. Arda, M. Yuksel, and N. Kabay, "Influence of the chosen process parameters on the efficiency of seawater desalination: Swro pilot plant results at urla bay seashore," *Desalination and Water Treatment - DESALIN WATER TREAT*, vol. 5, pp. 167–171, 05 2009.

[10] Y.-L. Li and K.-L. Tung, "Cfd simulation of fluid flow through spacer-filled membrane module: selecting suitable cell types for periodic boundary conditions," *Desalination*, 2008, the Fourth Conference of Aseanian Membrane Society: Part 1.

[11] M. S. Dodd, P. Trefftz-Posada, and A. Ferrante, "A coupled volume-of-fluid/pressure-correction method for incompressible gas-liquid flows with phase change," *Journal of Computational Physics*, vol. 539, p. 114252, 2025.

[12] S.-C. Tsai, W.-Z. Huang, G.-S. Lin, Z. Wang, K.-L. Tung, and C.-J. Chuang, "Evaluation of the specific energy consumption of sea water reverse osmosis integrated with membrane distillation and pressure–retarded osmosis processes with theoretical models," *Membranes*, vol. 12, no. 4, 2022.

[13] B. Amos, L. Xu, and J. Z. Kolter, "Input convex neural networks," *CoRR*, vol. abs/1609.07152, 2016. [Online]. Available: http://arxiv.org/abs/1609.07152

[14] A. Ruiz-García and I. de la Nuez-Pestana, "A computational tool for designing bwro systems with spiral wound modules," *Desalination*, vol. 426, pp. 69–77, 2018.

[15] S. Sablani, S. Al-Maskari, R. Al-Belushi, and M. Wilf, "Effect of feed temperature on permeate flux and mass transfer coefficient in spiral-wound reverse osmosis systems," *Desalination*, vol. 144, pp. 367–372, 09 2002.

979-8-3315-8138-1